The role of apical oxygen in the high-temperature superconductors

1996 J. Phys.: Condens. Matter 8 11053

(http://iopscience.iop.org/0953-8984/8/50/029)

J. Phys.: Condens. Matter **8** (1996) 11053–11068. Printed in the UK

The role of apical oxygen in the high-temperature superconductors

Carmine Lubritto†, Krzysztof Rościszewski‡ and Andrzej M Oleś‡

† Dipartimento di Fisica Teorica e SMSA, Universita' di Salerno—INFM Unita' di Salerno, I-84081 Baronisi, Salerno, Italy

‡ Institute of Physics, Jagellonian University, Reymonta 4, PL-30059 Kraków, Poland

Received 12 February 1996, in final form 12 September 1996

Abstract. We report finite-cluster diagonalizations which clarify the role of apical oxygen orbitals and of the copper $d_{3z^2-r^2}$ orbitals in the ground-state electronic properties of high-temperature superconductors. The hole density distribution and spin–spin correlation functions are analysed as functions of interoxygen hopping and other parameters. The main conclusion is that for universally accepted parameters for CuO_2 planes, small levels of doping and no phonons, the three-band Hamiltonian suffices to describe the properties of the ground state and the inverse photoemission.

1. Introduction

In spite of extensive theoretical and experimental studies, the electronic structure of high-T_c superconducting oxides (HTSO) is still not fully understood. It is commonly accepted that the electron transport and the physical processes leading to superconductivity originate from the partially occupied electronic states within the CuO_2 planes. Several experiments performed on the HTSO indicate anomalous behaviour and are hard to explain using band-structure calculations, or other implications of the independent-electron approximation. The importance of hole correlations at Cu orbitals is manifested by the fact that the undoped parent high-T_c compounds are charge-transfer insulators with a band gap of between 1.5 and 2.0 eV, and exhibit an antiferromagnetic (AF) long-range order (LRO) in the ground state. In contrast, the local density approximation (LDA) calculations [1, 2] predict that the undoped La_2CuO_4 and $YBa_2Cu_3O_6$ are nonmagnetic metals. The AF LRO may be easily understood in the ionic limit by occupying the $3d^9$ ($3d_{x^2-y^2}$ hole) configurations of Cu ions in the undoped system. Due to the strong Coulomb repulsion between the holes at Cu sites, the extra holes introduced by doping reside primarily on oxygen sites, as shown by various spectroscopic experiments [3, 4]. This is another consequence of electron correlations and at the same time an explanation of why LDA (except for the LDA$+U$ approach [5]) cannot work for these systems, and one has to use a many-body approach instead.

The theoretical challenge is to find the simplest model of the copper–oxygen plane which would contain all the essential physical aspects. The electronic structure calculations suggest [1, 2] that a good starting point is provided by the so-called three-band model [6, 7], including copper $3d_{x^2-y^2}$ orbitals and oxygen $2p_\sigma$ orbitals. However, it has been pointed out [8] that for a realistic description of the principal features of the cuprate superconductors, like for example the insulating gap in the undoped parent compounds, one has to include

0953-8984/96/5011053+16$19.50

also the orbitals of apical oxygens. The differences between various HTSO result from either octahedra, or pyramids or squares composed by oxygen ions surrounding a central copper ion of the CuO_2 plane.

Several experiments indicate that the out-of-plane apical oxygen orbitals are also involved in accommodating some of the holes doped into CuO_2 planes [9, 10]. In addition, various mechanisms of superconductivity have been proposed in which the $3d_{3z^2-r^2}$ orbitals play an essential role [11–13]. Furthermore, there is evidence that the apical oxygens modify the electronic structure in a way that is important for superconductivity. For example, a significant isotope effect has been observed for the apical oxygen [14], and there exists a clear correlation between a maximum critical temperature T_c^{max} reached in different cuprates and the copper-to-apex bonding [15], as well as the Madelung potential at the apical oxygen measured with respect to that at the oxygens in the planes [16]. This motivates the use of the five-band model introduced in [16–18]. Furthermore, it became clear recently that such an extended model which includes the apical oxygen orbitals is inevitable if one wants to account for the differences between the values of the maximal transition temperature T_c^{max} in different cuprates, using an effective single-band model which reproduces the low-energy scale [19].

The oxygen orbitals in the CuO_2 plane combine to two local symmetries which hybridize either with $3d_{x^2-y^2}$ or with $3d_{3z^2-1}$, respectively: the b_1 symmetry $\frac{1}{2}(p_x - p_y - p_{-x} + p_{-y})$, and the a_1 symmetry $\frac{1}{2}(p_x + p_y - p_{-x} - p_{-y})$, assuming the commonly used convention for the orbital phases [20]. As Zhang and Rice pointed out [20], a hole in a copper $d_{x^2-y^2}$ orbital and a hole in the b_1-symmetry oxygen orbital form a local singlet for the realistic parameters, and the three-band model does reduce to an effective single-band t–J model. Such a mapping may break down, however, if the triplet states stabilized by the occupancy of apical oxygen p_a and copper $d_{3z^2-r^2}$ orbitals are energetically close to the Zhang–Rice (ZR) singlets [21]. Therefore, it is important to investigate the value of the splitting between the lowest singlet and triplet states, and under what circumstances this splitting decreases.

Following this motivation, we investigate here the role of the copper $d_{3z^2-r^2}$ and apical oxygen p_a orbitals in the electronic structure of the CuO_2 plane. Our first aim is to study the ground state in order to: (i) determine the filling of $d_{3z^2-r^2}$ and apical oxygen p_a orbitals, and (ii) establish the role of such electronic structure parameters as interoxygen hoppings which determine the covalency, t_{pp} and t_{pa}, the bare atomic level energy ε_a at the apical oxygen, and, finally, the crystal-field splitting ε_z between the copper $d_{x^2-y^2}$ and $d_{3z^2-r^2}$ orbitals, in the formation and stability of the ZR singlets. Furthermore, it is of interest to investigate the AF correlations for the ground states of both undoped and doped copper–oxygen clusters, even realizing that information gained from small cluster calculations is somewhat limited. We also studied the excited states in order to find out whether the states of a_1 symmetry might be observed in low-energy photoemission.

The paper is organized as follows. In section 2 we introduce the five-band Hamiltonian and discuss its parameters. Section 3 is devoted to the presentation of numerical results obtained for the ground state of CuO_6 and Cu_2O_{11} clusters. These results are compared with other theoretical and experimental results. A summary and final conclusions are given in section 4.

2. The five-band model

The five-band extended Hubbard model for the electronic states of CuO_2 planes of the HTSO consists of the following orbitals: $d_{x^2-y^2}$ (x-) and $d_{3z^2-r^2}$ (z-) orbitals for copper

atoms, the bonding p_σ, i.e. $2p_x$ and $2p_y$, orbitals (p) for oxygen atoms in the plane (along the bands) and the $2p_z$ orbitals (a) for the out-of-plane apical oxygen ions. Using the simplified notation where we call the orbitals involved x, z, p, and a, respectively, the Hamiltonian of the five-band model reads

$$\begin{aligned} H = & \sum_{m,\alpha\sigma} \varepsilon_\alpha n_{m,\alpha\sigma} + \varepsilon_p \sum_{i,\sigma} n_{i,p\sigma} + \varepsilon_a \sum_{k,\sigma} n_{k,a\sigma} + \sum_{\langle m,i\rangle,\alpha\sigma} t_{\alpha p}(d^\dagger_{m,\alpha\sigma} p_{i\sigma} + \text{HC}) \\ & + t_{za} \sum_{\langle m,k\rangle,\sigma} (d^\dagger_{m,z\sigma} a_{k\sigma} + \text{HC}) + t_{pp} \sum_{\langle i,j\rangle,\sigma} (p^\dagger_{i\sigma} p_{j\sigma} + \text{HC}) \\ & + t_{pa} \sum_{\langle i,k\rangle,\sigma} (p^\dagger_{i\sigma} a_{k\sigma} + \text{HC}) \\ & + U_d \sum_{m\alpha} n_{m,\alpha\uparrow} n_{m,\alpha\downarrow} + U_p \sum_i n_{i,p\uparrow} n_{i,p\downarrow} + U_a \sum_k n_{k,a\uparrow} n_{k,a\downarrow} \\ & + \left(U_{xz} - \frac{1}{2} J_{xz}\right) \sum_m n_{mx} n_{mz} + J_{xz} \sum_m (d^\dagger_{m,x\uparrow} d^\dagger_{m,x\downarrow} d_{m,z\downarrow} d_{m,z\uparrow} + \text{HC}) \\ & - 2J_{xz} \sum_m \boldsymbol{S}_{mx} \cdot \boldsymbol{S}_{mz} + \sum_{\langle m,i\rangle,\alpha} U_{\alpha p} n_{m\alpha} n_{ip} + \sum_{\langle m,k\rangle,\alpha} U_{\alpha a} n_{m\alpha} n_{ka}. \end{aligned} \tag{1}$$

Here the $d^\dagger_{m,x\sigma}$ and $d^\dagger_{m,z\sigma}$ ($d_{m,x\sigma}$ and $d_{m,z\sigma}$) are hole creation (annihilation) operators in the orbitals $d_{x^2-y^2}$ and $d_{3z^2-r^2}$ at copper ions, respectively, the $p^\dagger_{i\sigma}$ stand for the p_σ ($2p_x$ and $2p_y$) orbitals at oxygen sites in CuO_2 planes, while the $a^\dagger_{k\sigma}$ refer to the apical oxygen orbitals. Furthermore, $\boldsymbol{S}_{mx}$ and $\boldsymbol{S}_{mz}$ are the corresponding hole spin operators for a hole in one of the copper orbitals. The hole number operators are defined in a standard way, e.g., $n_{m,\alpha\sigma} = d^\dagger_{m,\alpha\sigma} d_{m,\alpha\sigma}$, $n_{m\alpha} = \sum_\sigma n_{m,\alpha\sigma}$ for the copper orbitals, with $\alpha = x, z$, etc. The sums over the respective nearest-neighbour pairs of a given type are indicated by $\langle ij\rangle$. For convenience, we have indicated the summations over the copper, in-plane oxygens, and apical oxygens by m, i (j), and k, respectively.

The first three terms of (1) specify the reference hole atomic energies: ε_x, ε_z, ε_p, and ε_a, for the different types of orbital. The hopping elements $t_{\alpha p}$ ($\alpha = x, z$), t_{za}, t_{pp}, and t_{pa} stand for the copper–oxygen, oxygen–oxygen-in-plane, and oxygen-in-plane–apical-oxygen hopping, respectively. The on-site intraorbital Coulomb interactions are described by U_d-, U_p- and U_a-elements, while the interorbital Coulomb and exchange elements at Cu sites are defined as U_{xz} and J_{xz}. Only the most important intersite Coulomb interactions between nearest-neighbour copper and oxygen sites, U_{dp} and U_{da}, are included in (1).

For convenience we are using the hole notation throughout the paper. The orbital wave functions were chosen to be real and we follow the same phase convention as in [20]. We fixed the phases of the apical oxygens by assuming a local mirror symmetry plane which results in the same signs of the hopping elements connecting the $3d_{z^2-r^2}$ orbital and upper (lower) apical oxygen. Note that the phases were not explicitly included in equation (1), to simplify the notation. The vacuum of Hamiltonian (1) is defined by the $3d^{10}2p^6$ configuration. With respect to this state we are interested in: (i) the two-hole solution describing the doped system in the simplest Cu_1O_6 cluster; (ii) the two-, three-, and four-hole solutions describing the undoped, doped and overdoped systems for the Cu_2O_{11} (Cu_2O_9) cluster, respectively.

The ground state of the multiband model Hamiltonian (1) depends on the actual values of the parameters. In order to represent the holes within CuO_2 planes which include the apical oxygens, we have used the parameter set given by Grant and McMahan [8] (see the 'realistic' parameters in table 1). They were determined from the LDA calculations by using

Table 1. Various sets of parameters of Hamiltonian (1) (in eV) used in the calculations.

	Realistic set [8]	Ovchinnikov set [39]	Three-band model
ε_x	0.00	0.00	0.00
ε_z	0.64	9.64	9.64
ε_p	3.51	3.51	3.51
ε_a	2.05	9.05	9.05
t_{xp}	1.30	1.30	1.30
t_{zp}	0.75	0.75	0.00
t_{za}	0.82	0.00	0.00
t_{pp}	0.65	0.65	0.00
t_{pa}	0.33	0.00	0.00
U_{dd}	8.96	8.96	8.96
U_{xz}	6.58	6.58	0.00
J_{xz}	1.19	1.19	0.00
U_p	4.19	4.19	4.19
U_a	3.67	3.67	3.67
U_{xp}	0.52	0.52	0.00
U_{zp}	0.52	0.52	0.00
U_{xa}	0.18	0.18	0.00
U_{za}	0.18	0.18	0.00

a 'fixed-charge' method, as described in [22]. We note that quite similar parameters were obtained also from other LDA calculations [23], and from a combination of spectroscopic data, *ab initio* results and some scaling arguments [24, 25].

In table 1 we have also included the three-band model parameters. Using this set of parameters one can reduce the five-band model (1) to the three-band model [6, 7]:

$$H = \varepsilon_d \sum_{m\sigma} d^\dagger_{m\sigma} d_{m\sigma} + \varepsilon_p \sum_{i\sigma} p^\dagger_{i\sigma} p_{i\sigma} + t_{dp} \sum_{\langle i,j\rangle,\sigma} (d^\dagger_{m\sigma} p_{i\sigma} + \text{HC}) + U_d \sum_m n_{m,d\uparrow} n_{m,d\downarrow} + U_p \sum_i n_{i,p\uparrow} n_{i,p\downarrow} + U_{dp} \sum_{\langle m,i\rangle,\sigma,\tau} n_{m,d\sigma} n_{i,p\tau}. \quad (2)$$

Here we have used the commonly used notation for the charge-transfer model, with $d_{m\sigma}$ and $n_{m,d\sigma}$ standing for the respective hole operators for the $3d_{x^2-y^2}$ orbitals at Cu sites, and ε_d for the hole energy at copper sites.

In order to make a systematic study to investigate the influence of the apical oxygens on the electronic structure, and their role in covalency, we determined the ground state and first excited states of the five-band model (1) for different values of ε_a, t_{pp} and t_{pa}. The many-body problem posed by Hamiltonian (1) was solved by numerical diagonalization. The size of the matrix could be reduced by using a few symmetries of the Hamiltonian which commutes both with the total hole number operator, and with the operator of the z-component of the total spin. We used the exact diagonalization for the CuO_6 cluster, while the results for the larger clusters were obtained using the Lanczos method [26–29].

The ground states obtained in the various situations considered have been analysed by calculating: (i) the excitation energies of the lowest excited states; (ii) the hole density distribution $\langle n_{i,\alpha\sigma}\rangle$ for the copper and oxygen orbitals; and (iii) spin–spin correlation

functions, defined in the usual way:

$$\langle \boldsymbol{S}_{i\alpha} \cdot \boldsymbol{S}_{j\beta} \rangle = -\frac{1}{2} \langle c^{\dagger}_{i,\alpha\uparrow} c_{j,\beta\uparrow} c^{\dagger}_{j,\beta\downarrow} c_{i,\alpha\downarrow} + c^{\dagger}_{j,\beta\uparrow} c_{i,\alpha\uparrow} c^{\dagger}_{i,\alpha\downarrow} c_{j,\beta\downarrow} \rangle + \frac{1}{4} \langle n_{i,\alpha\uparrow} n_{j,\beta\uparrow} + n_{i,\alpha\downarrow} n_{j,\beta\downarrow} - n_{i,\alpha\uparrow} n_{j,\beta\downarrow} - n_{i,\alpha\downarrow} n_{j,\beta\uparrow} \rangle. \tag{3}$$

Here the spin operators $\boldsymbol{S}_{i\alpha} = \frac{1}{2} \sum_{\tau\sigma} c^{\dagger}_{i,\alpha\sigma} \boldsymbol{\sigma}_{\sigma\tau} c_{i,\alpha\tau}$, the $\boldsymbol{\sigma}$ are the Pauli matrices, and the $c_{i,\alpha\sigma}$ each stand for one of the operators: $d_{i,x\sigma}$, $p_{i\sigma}$, or $a_{i\sigma}$ (as appropriate), where i labels the site in the cluster and $\alpha, \beta = x, z, p, a$ are the orbital indices ($\alpha \neq \beta$).

The spin–spin correlation functions are nontrivial, and were analysed with special attention. We have determined, for various dopings (i.e., for different numbers of holes in the cluster), the spin–spin correlation function (3) in the Cu_2O_{11} cluster connecting the two copper spins within $d_{x^2-y^2}$ orbitals, S_{xx}; and that connecting the copper $d_{x^2-y^2}$ hole and the hole on the bridge oxygen (which is representative of the respective spin–spin, copper–oxygen b_1-symmetry-type correlation in the infinite system), S_{xp}. The other spin–spin correlation functions were found to be very small for realistic parameters due to the low occupancy of $d_{3z^2-r^2}$ and apical orbitals, and will not be considered further.

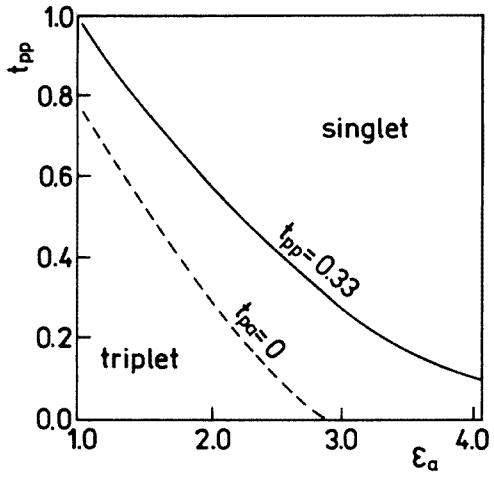

Figure 1. The singlet–triplet phase diagram on the (t_{pp}, ε_a) plane, as obtained for a Cu_1O_6 cluster filled by two holes for the realistic parameters, given in table 1. The solid (dashed) line corresponds to $t_{pa} = 0.33$ eV ($t_{pa} = 0$).

3. Numerical results

3.1. The ground state of the Cu_1O_6 cluster

We start our analysis with a Cu_1O_6 cluster filled by two holes. One finds that depending on the values of the energy of the apical oxygen orbital ε_a, and on the value of the interoxygen hopping parameter t_{pp}, the ground state is either a ZR singlet [20], or a triplet, as shown in figure 1. In fair agreement with Fujimori [30], we find a singlet ground state when the extra hole is in a b_1-symmetry ($d_{x^2-y^2}$-like) molecular orbital composed of the in-plane oxygen orbitals, and makes the bonding with the opposite spin within the Cu ($3d_{x^2-y^2}$) orbital.

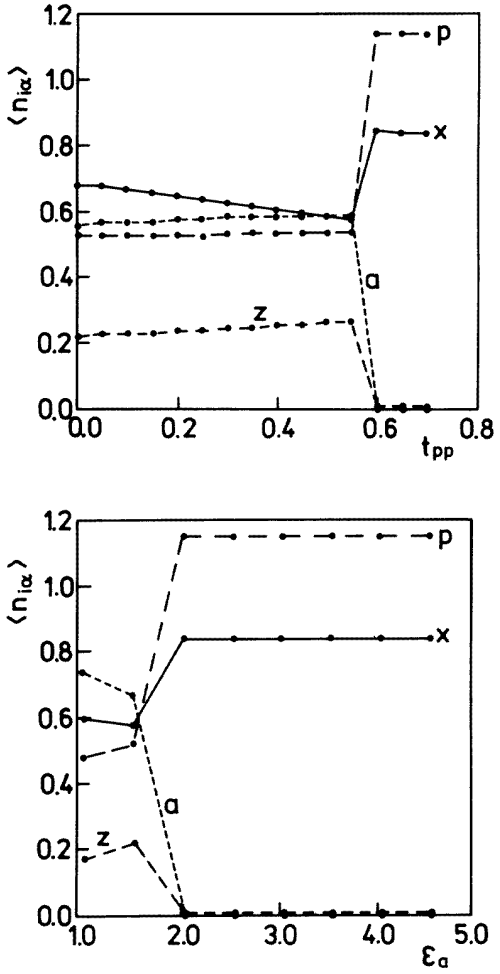

Figure 2. Hole densities $\langle n_{i\alpha}\rangle$ for a Cu_1O_6 cluster filled by two holes for the realistic parameters, as functions of the interoxygen hopping, t_{pp} (top), and of the apical orbital energy ε_a (bottom). Solid, long-dashed, medium-dashed, and dotted lines correspond to the hole numbers within $d_{x^2-y^2}$ (x-), p_σ (p), $d_{3z^2-r^2}$ (z-), and p_a (a-) orbitals, respectively.

The two states have drastically different hole distributions, as shown in figure 2. In the region of the ZR singlet in the phase diagram one finds that *only the planar oxygen p_σ and copper $d_{x^2-y^2}$ orbitals are important*. In this case the doping occurs mainly on the oxygen orbitals within the plane. In contrast, the triplet ground state is characterized by *significant occupation numbers for all of the orbitals in the cluster*. This shows that the doped hole (with respect to the one-hole state which stands for the undoped system) occupies the a_1-symmetry state, and the molecular triplet (instead of a singlet) is stabilized by the on-copper exchange interaction J_{xz}. In fact, the triplet region is considerably decreased for $J_{xz} = 0$.

As expected, increasing ε_a stabilizes the ZR singlet state, while the triplet state is stable for $\varepsilon_a < 1.7$ eV (see figure 1). This finding is in perfect agreement with the earlier results of Eskes *et al* [31], and Fujimori [30]. The crossover to the triplet state is accompanied by a drastic redistribution of hole density, with almost one hole occupying the a_1-symmetry

($3d_{3z^2-r^2}$ and $2p_a$) states (see the lower panel of figure 2). Furthermore, the ZR singlet is stabilized by the interoxygen hopping due to its stronger contribution to the bonding in this state. In contrast, the triplet is stabilized by increasing the in-plane–apex-oxygen hopping t_{pa}, as shown by the transition lines for $t_{pa} = 0$ and $t_{pa} = 0.33$ eV in the $\{\varepsilon_a, t_{pp}\}$ phase diagram of figure 1. We have verified that the hole density decreases within the apical orbitals with decreasing t_{pa}.

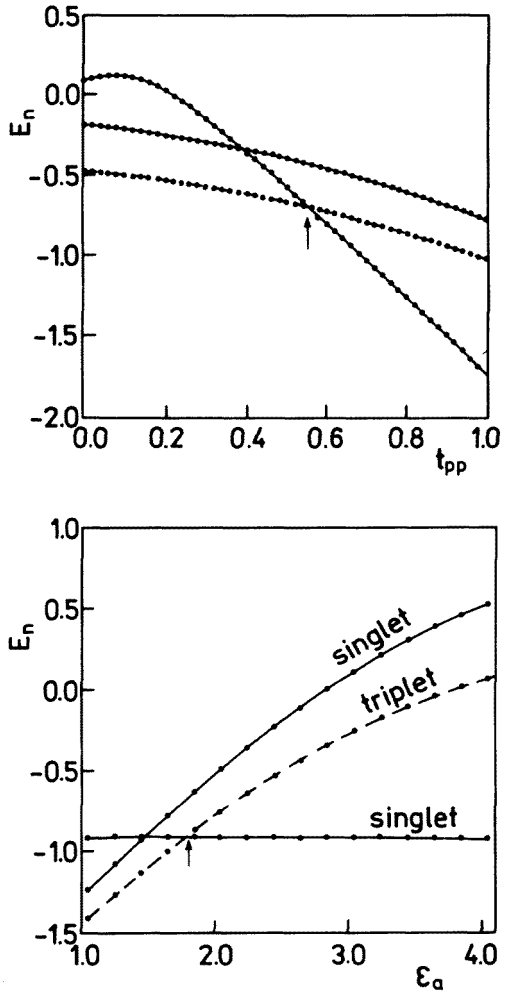

Figure 3. The energies (E_n) of the lowest-energy states of b_1-symmetry singlet (the Zhang–Rice singlet, solid line), and of a_1-symmetry triplet (dashed line) and singlet states, as obtained for a Cu_1O_6 cluster filled by two holes by varying interoxygen hopping t_{pp} (top) and the apical orbital energy ε_a (bottom); the other parameters are from the realistic set (see table 1). Arrows indicate the point of crossover between the ZR singlet and a_1-triplet ground state.

We note that for the realistic parameters of [8] one finds a singlet ground state for the CuO_6 cluster. The singlet–triplet excitation energy, shown in figure 3, is relatively small in the regime investigated. We emphasize that the singlet–triplet transition presented in figures 1–3 results from the competition between the b_1 (ZR) singlet stabilized by the $x-p$

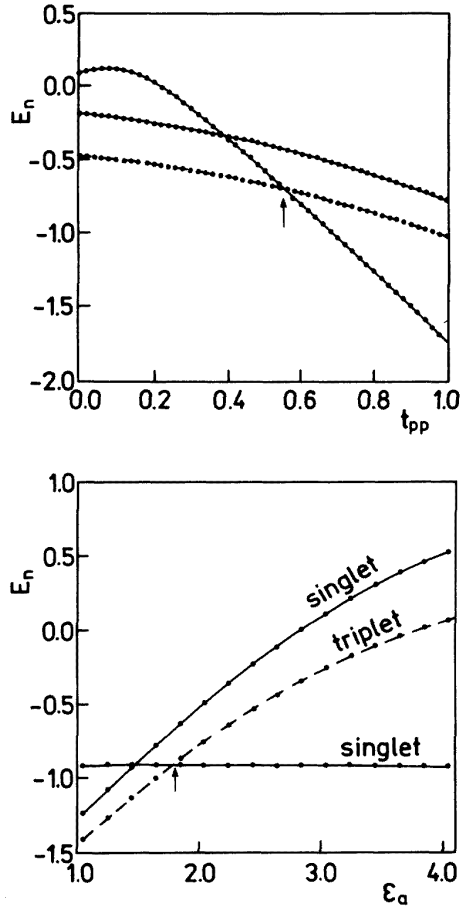

Figure 4. Singlet (solid line) and triplet (dashed line) energies versus interoxygen hopping t_{pp}, as obtained for a Cu_1O_6 cluster filled by two holes; the parameters are from the Ovchinnikov set (see table 1).

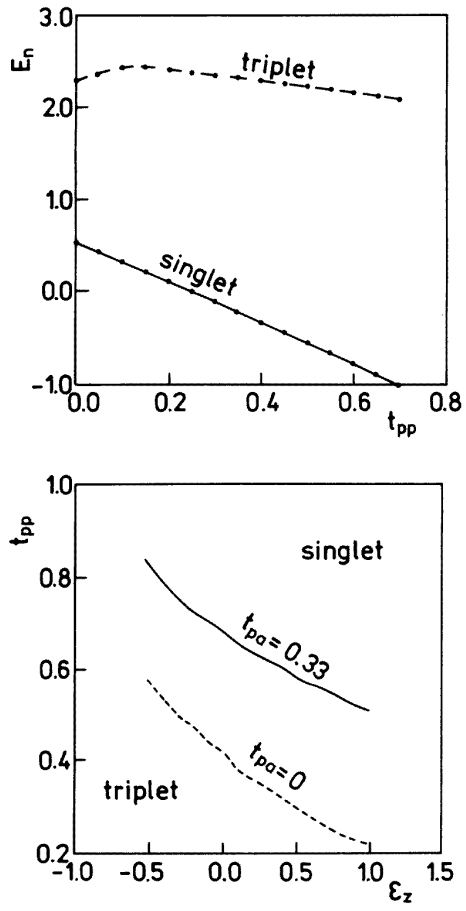

Figure 5. The singlet–triplet phase diagram on the (t_{pp}, ε_z) plane, as obtained for the Cu_1O_6 cluster filled by two holes with the realistic set of parameters.

covalency, and the a_1 singlet stabilized by Hund's rule. Instead, Ovchinnikov claimed that a different triplet state of b_1 symmetry might be stabilized by the increasing interoxygen hopping t_{pp} [32]. In order to reproduce the physical situation studied in [32], we considered two holes within the CuO_6 cluster using the restricted b_1 subspace, putting in the bare atomic levels of $d_{3z^2-r^2}$ and apical oxygen orbitals, ε_z and ε_a at high energies (over 9 eV), and assuming no hybridization between the orbitals of different (b_1 and a_1) symmetry. Using the set of parameters as given in table 1, one finds no crossover between the singlet and (b_1) triplet when the covalency t_{pp} is varied (figure 4). Even a small value of the intersite exchange interaction between d and p orbitals of the three-band model (considered in [32]) is not able to change our qualitative conclusion that the singlet–triplet splitting within the subspace of states of b_1 symmetry is large, and in fact *the increasing covalency t_{pp} stabilizes* the ZR singlet further. Thus, there is no new ferromagnetic contribution in a CuO_6 cluster, linear in the covalency and promoted by the p–p hopping, contrary to the conclusion of [32].

Our study of the ground state of the CuO_6 cluster is completed by considering the role

of the crystal-field splitting ε_z. It is found that the a_1 triplet is stabilized by the decreasing value of ε_z as shown by the phase diagram in the $\{\varepsilon_z, t_{pp}\}$ plane presented in figure 5. This dependence is quite strong, and, for instance, without the crystal-field splitting ($\varepsilon_z = 0$) the ground state is an a_1 triplet for the realistic values of t_{pp} and t_{pa} (see figure 5). This demonstrates the importance of the copper $d_{3z^2-x^2}$ orbital in the stabilization of the a_1-triplet state. The participation of the $d_{3z^2-x^2}$ orbital in the triplet ground state follows also from the increasing triplet stability with the increasing value of t_{pa}.

3.2. The ground state of the Cu_2O_{11} cluster

Such qualitative trends as the increasing role of the a_1-symmetry states with either a decreasing value of the crystal-field splitting ε_z, or with an increasing t_{za}-hopping, are also observed for the larger Cu_2O_{11} cluster. Our purpose is to demonstrate to what extent the larger covalency between the orbitals within the CuO_2 plane favours the b_1 states.

We have analysed the ground state of a Cu_2O_{11} cluster filled by $N = 3$ holes as a function of: (i) the interoxygen hopping t_{pp}; and (ii) the apical oxygen energy ε_a in the doped case. The ground state appears to be always a low-spin ($S = 1/2$) state in the region of model parameters investigated, but one finds two different ground states when the interoxygen hopping t_{pp} is varied, corresponding to the above-discussed ground states of the CuO_6 cluster with $N = 2$ holes. While the two holes of the undoped Cu_2O_{11} cluster occupy the b_1 states, the added hole has predominantly a_1 character, if $t_{pp} \leqslant 0.35$ eV (see figure 6). In this case the local components of the triplet discussed above for the CuO_6 cluster dominate and combine with the remaining down-spin hole to form a low-spin state. Thus, the spin compensation is nonlocal for small t_{pp}. In contrast, the other ground state stabilized by $t_{pp} \geqslant 0.35$ eV is dominated by the local components of ZR singlets, which combine again with the remaining up-spin hole on the other site. As in the earlier studies [16, 30, 33], we have found that the ground state in the Cu_2O_{11} cluster is well represented by a 'bonding' state of two components with (local) ZR singlets formed around the copper holes in the realistic range of parameters. The transition between the two different ground states is of first-order type.

As found by Ohta *et al* [16], the first excited state for the realistic parameters is mainly represented by the 'anti-bonding' state of the two ZR singlets. This picture is also confirmed by the results obtained for the clusters with apical oxygens. The measure of stability of local singlets is given by $2|t|$ [33], with the effective hopping $t \simeq 0.5$ eV [16, 33], and decreases with decreasing values of either t_{pp}, or ε_a, in fair agreement with the work of Eskes *et al* [33].

We have found that the stability of the ground state with the ZR singlet components is influenced strongly by other (mainly triplet) components involved in the first-excited state. The crossover to a ground state with large triplet components is accompanied by the change of the first-excited state, which contains then the triplet components instead of the anti-bonding combination of two local singlets at either site, in agreement with the earlier result of Tohyama and Maekawa [34]. Such a crossover could be identified not only for a decreasing value of interoxygen hopping in the plane (figure 6), but also for a decreasing value of the bare atomic level ε_a (see figure 7). Altogether, this allows one to conclude that the local ZR singlets are stabilized by their covalency between the copper and in-plane oxygen orbitals, if the energy of apical oxygen orbitals is not too low, which supports the earlier findings by Ohta *et al* [16].

The changes in the hole density distribution with varying apical oxygen level energy ε_a can be followed in detail in figure 7. As expected, the occupancy of the apical oxygen

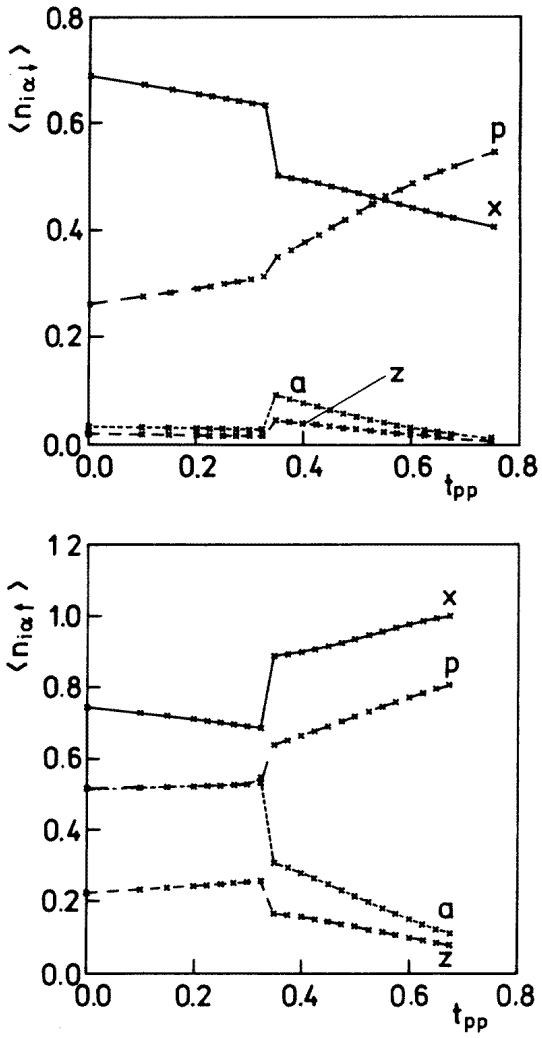

Figure 6. Hole ↓-spin $\langle n_{i\alpha\downarrow}\rangle$ (upper) and ↑-spin $\langle n_{i\alpha\uparrow}\rangle$ (lower) hole densities for the Cu_2O_{11} cluster filled by three (two ↑-spin and one ↓-spin) holes for the realistic parameters of table 1, as functions of the interoxygen hopping, t_{pp}. Solid, long-dashed, medium-dashed, and dotted lines correspond to the hole numbers within $d_{x^2-y^2}$, p_σ, $d_{3z^2-r^2}$, and p_a orbitals, respectively.

orbitals p_a increases with decreasing ε_a which reflects the increasing component of the local triplets in the ground state. But more importantly, the crossover to the ground state dominated by the local triplet components occurs here in a continuous way, unlike in the case of decreasing covalency t_{pp} (see figure 6). The more localized character of the triplet components at low values of ε_a is demonstrated by the increased (decreased) $d_{x^2-y^2}$ ($2p_\sigma$) density of the down-spin hole in figure 7. We note that the occupancy changes due to the variation of ε_a are in fair agreement with the results of the slave-boson treatment of the five-band model by Feiner, Grilli, and Di Castro [18].

The hole density distributions for the undoped and doped Cu_2O_9 and Cu_2O_{11} clusters and for the realistic parameters for CuO_2 planes [8] are summarized in table 2. In the

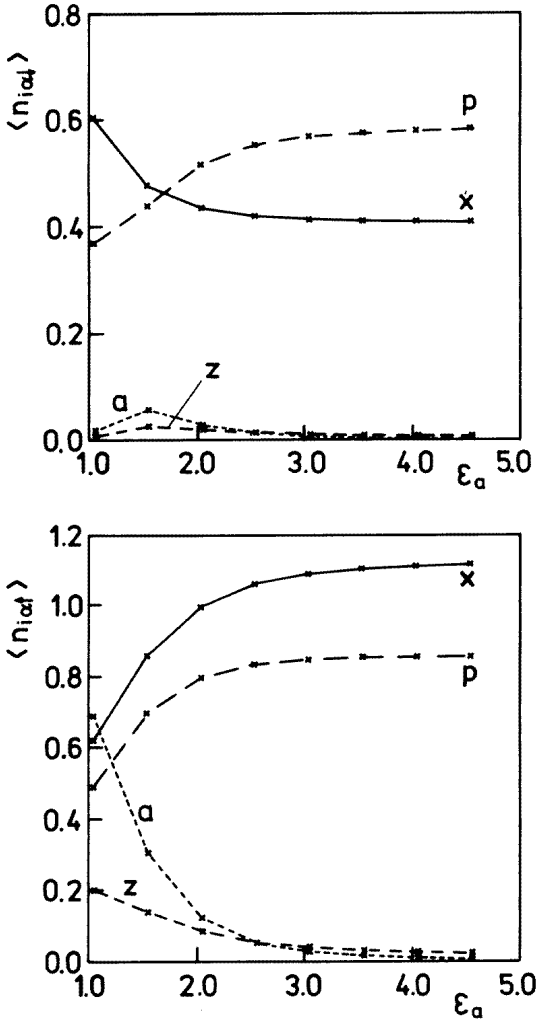

Figure 7. As figure 6, but for varying apical orbital energy ε_a.

undoped system ($N = 2$) one finds that the a_1 orbitals are unoccupied and that the hole density at Cu ($3d_{x^2-y^2}$) and O ($2p_\sigma$) orbitals is 0.67 and 0.33, respectively. This density distribution practically reproduces the earlier results obtained by exact diagonalization for the Cu_4O_8 cluster with periodic boundary conditions [35, 36], and by local *ansatz* method for a nonmagnetic and AF state of the CuO_2 plane [37, 38]. On comparing these fillings with those for the doped systems (see table 2), we note that the largest increase of hole density under doping occurs in the planar oxygen orbitals p_σ, reflecting the well known fact that due to the strong Coulomb repulsion U_d at copper ions the doped holes go mainly to oxygen sites [37], and lead to the formation of ZR singlets [20].

The apical orbitals are partly occupied by the doped hole, with about 4% of a hole coming to both (initially empty) $3d_{3z^2-r^2}$ and $2p_a$ orbitals in the Cu_2O_9 cluster, and considerably larger fillings of 10.6% and 15.5%, respectively, in the Cu_2O_{11} cluster (see table 2). This demonstrates once again that a stronger covalency of a_1 states in the Cu_2O_{11}

Table 2. Hole densities within $d_{x^2-y^2}$, $d_{3z^2-r^2}$, p_σ, and p_a orbitals in Cu_2O_9 and Cu_2O_{11} clusters for the realistic parameters of high-T_c superconductors (table 1), and for various total numbers of holes $N = 2$, 3, and 4.

		$N=2$	$N=3$			$N=4$
Cluster	Orbital	$\langle n_i \rangle$	$\langle n_{i\uparrow} \rangle$	$\langle n_{i\downarrow} \rangle$	$\langle n_i \rangle$	$\langle n_i \rangle$
Cu_2O_9	$d_{x^2-y^2}$	1.334	1.096	0.413	1.509	1.602
	$d_{3z^2-r^2}$	0.002	0.030	0.009	0.039	0.082
	p_σ	0.662	0.841	0.569	1.410	2.072
	p_a	0.002	0.032	0.009	0.041	0.244
Cu_2O_{11}	$d_{x^2-y^2}$	1.330	0.994	0.435	1.429	1.293
	$d_{3z^2-r^2}$	0.004	0.086	0.020	0.106	0.353
	p_σ	0.663	0.796	0.514	1.310	1.548
	p_a	0.003	0.124	0.031	0.155	0.806

cluster increases their hole occupancy. In this latter case the fraction of holes on copper $d_{3z^2-r^2}$ orbitals amounts to about 3.5% of the total number of holes in the cluster, i.e. to about 7% of the hole count at oxygen sites. These results are in fair agreement with the experimental results of Pellegrin *et al* [39], and Chen *et al* [10], who found that the fraction of apical oxygen holes and copper $d_{3z^2-r^2}$ holes is close to 10% and $3 \pm 3\%$ respectively (for $x = 0.3$, where x is the dopant concentration).

The clusters filled by $N = 4$ holes in table 2 represent the highly overdoped regime. First of all, the density of holes within the a_1-symmetry states in then much enhanced with respect to the clusters filled by $N = 3$ holes. Again, the role of covalency within the a_1 subset of states is reflected in the strong increase of the a_1-hole count, from $\sim$0.08 and $\sim$0.24 to $\sim$0.35 and $\sim$0.81, by going from the Cu_2O_9 to Cu_2O_{11} cluster, respectively. Secondly, by studying the energy spectra as functions of t_{pp} and ε_a (not shown), one finds that the triplet excited state is quite close to the singlet ground state for a broad range of parameters, with no crossing of these two energies. Analysing the occupancies one can identify the same two regions of behaviour as described above for $N = 3$ holes. The only qualitative difference was found for the Cu_2O_{11} cluster, where the largest component of the ground state contains a single ZR singlet, while the second hole occupies predominantly the apical oxygen orbitals p_a ($\sim$0.4 of a hole per spin).

The different magnetic properties of the ground states of Cu_2O_{11} clusters are best illustrated by the spin–spin correlation functions (3) connecting the two copper sites, S_{xx}, and connecting a copper hole and the hole which occupies the neighbouring oxygen orbitals, S_{xp}, shown in figure 8. Both functions are AF over the whole parameter range investigated, but their strengths depend on the nature of the ground state obtained (see figure 8). The strong AF correlation between the copper sites at $N = 2$ follows just from the relatively high occupancy ($\sim$0.67 per site) of the $d_{x^2-y^2}$ orbitals (see table 2), while the small negative values of $|S_{xp}|$ follow from the weak covalency.

At $N = 3$ one finds a sharp crossover in the spin–spin correlations with increasing t_{pp}, which occurs at $t_{pp} \simeq 0.35$ eV, similar to that observed before for the density distribution (figure 6). For large (close to realistic) values of t_{pp}, S_{xx} goes to zero, while $|S_{xp}|$ becomes more negative. Thus, in this range of parameters the AF correlation between the two copper $d_{x^2-y^2}$ orbitals gradually disappears with increasing t_{pp}, and is replaced by the increasing AF correlation between the copper $d_{x^2-y^2}$ hole and the hole within the planar oxygen orbitals. This manifests the formation of the ZR singlet (local Kondo effect), accompanied by a

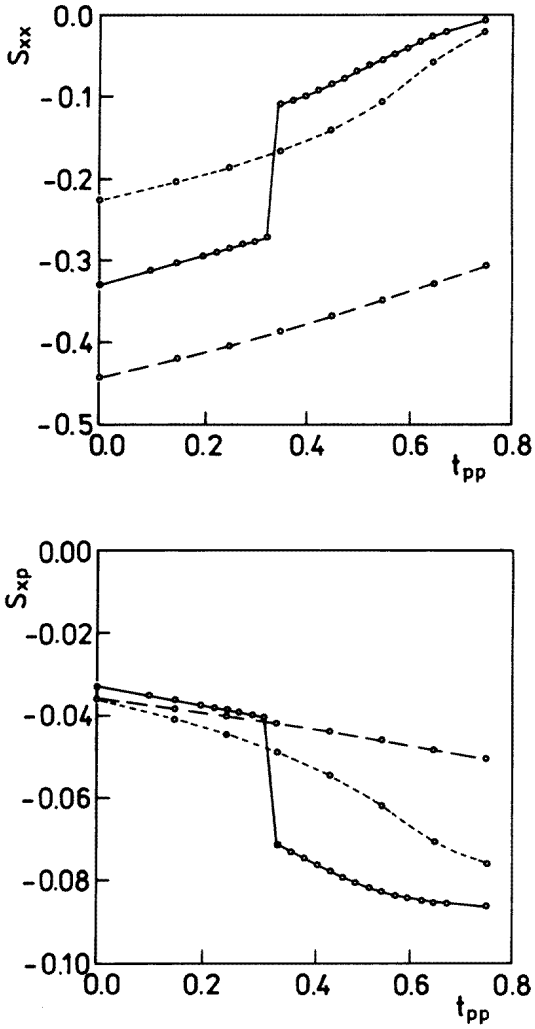

Figure 8. Spin–spin correlation functions: S_{xx} (top) and S_{xp} (bottom) versus interoxygen hopping t_{pp}, as obtained for the Cu_2O_{11} cluster with the realistic set of parameters (table 1). Long-dashed, solid, and short-dashed lines stand for the cluster filled by two, three, and four holes, respectively.

single hole on the second copper site. The local screening of the magnetic copper moment by the doped hole becomes more extended with increasing t_{pp}, and one finds that the correlation function S_{xx} becomes ferromagnetic for higher than realistic values of $t_{pp} > 0.8$ eV. This behaviour reflects the well known frustration of the magnetic interactions in the doped system [40]. In contrast, for $t_{pp} < 0.35$ eV one finds a ground state with significant occupancy of the a_1-symmetry orbitals, the copper $d_{3z^2-r^2}$, and the apical oxygen p_a orbitals (figure 6). As a result of nonlocal spin compensation the AF interactions between the copper sites are here more pronounced than those found for $t_{pp} > 0.35$ eV, but still weaker than in the undoped limit ($N = 2$). Finally, at $N = 4$ the spin–spin correlations change in a continuous way and are weaker than those at $N = 3$ for larger t_{pp}. Thus, the ZR singlet

component becomes screened out in the overdoped regime by the hole doped to the states of a_1 symmetry.

4. Summary and conclusions

The presented results of our finite-cluster calculations give evidence that the ZR singlets of a_1 symmetry compete with the local triplets of b_1 symmetry. This competition could be identified even in the smallest cluster considered: CuO_6 filled by two holes. It has been found that the stabilization of a singlet ground state and/or the increase of the singlet area of the phase diagram can be achieved in the five-band model by increasing either (i) ε_a, or (ii) t_{pp} (which enhances the in-plane covalency), or, finally, (iii) ε_z. In contrast, increasing the hopping element to the apical oxygens t_{pa} reduces the singlet area in the $\{\varepsilon_a, t_{pp}\}$ phase diagram. The above parameters have quite similar effects on the stability of b_1 and a_1 local states in larger clusters.

For the realistic parameters one finds that the singlet ground state is reproduced reasonably well by the three-band model—the apical oxygens p_a and the copper $d_{3z^2-r^2}$ orbitals might then be neglected in the naive model for CuO_2 planes, at least in the small-doping regime. For larger doping levels this is certainly not possible, as the triplet excited state is not well separated from the singlet ground state, and the stability of local singlets in the cluster is weak or even questionable. However, our calculations suggest that even in the low-doping regime the apical oxygen states play a role, as the parameters of the *effective* three-band model would depend on these degrees of freedom. Although such a model has not been derived explicitly so far, a similar situation is known for the effective t–t'–J model which depends sensitively on the a_1-symmetry states, renormalizing the effective next-nearest-neighbour hopping t' of doped holes [19, 41].

In agreement with the observed AF LRO, we found distinct AF correlation between copper spins for the undoped clusters. This correlation is suppressed by hole doping, where the strong local AF correlations between a hole on copper, and a second hole on the nearest-neighbour oxygens dominates for the realistic parameters. This reflects the formation of local ZR singlets, stable for the realistic parameters. But with decreasing t_{pp} and/or ε_a the local singlets are replaced by the local triplets, with significant occupancy of the apical oxygen orbitals. In this limit one finds a strong AF copper–copper correlation, while the in-plane copper–oxygen coupling becomes quite small. This crossover between the two different states may be viewed as a competition between the Kondo effect which stabilizes the ZR singlets, and the AF interactions between the copper spins which dominate only if the apical oxygens are occupied by doping.

We have also considered the spectral functions obtained for the undoped and doped CuO_6 and Cu_2O_{11} clusters. The results obtained confirm the generic picture of a charge-transfer insulator [42, 43], with two Hubbard subbands at low and high energies, and a broad nonbonding oxygen band in between. The insulating character of the undoped clusters follows from the Fermi level located within the charge-transfer gap. The spectra contain a highly correlated state close to the Fermi level which occurs due to the local excitations of ZR singlets, and becomes occupied by doping the Cu_2O_{11} cluster with one hole. One finds that the neighbouring low-energy maxima in the photoemission part of the spectral functions originate from apical oxygen p_a and copper $d_{3z^2-r^2}$ orbitals. Hence, we have to conclude that the three-band model reproduces well the inverse photoemission, while the realistic five-band model considered above is required to describe the photoemission spectra over a somewhat broader energy range.

We note that the number of holes in the apical oxygen orbitals increases with doping.

This has important consequences for the superconductivity, as it has been found that the superconductivity is suppressed by holes on apical oxygens [16, 19]. In this context it is interesting to reconsider the well known fact that the application of high pressure in the systems with apical oxygens raises the maximal value of the transition temperature into the superconducting state T_c (see the discussion in [16, 19]). This experimental fact appears to be consistent with our findings. First of all, high pressure decreases the bond lengths, which results in a small increase of interoxygen (t_{pp} and t_{pa}), and of copper–oxygen (t_{xp} and t_{zp}) hopping integrals. These effects compete with each other, as the increase of t_{pp} should strengthen the stability of the singlet ground state, while the increase of t_{pa} does the opposite, and the overall effect should be small. However, there are still other and much stronger effects. First of all, the four oxygens surrounding each copper come closer to the copper ion which is likely to increase the crystal-field splitting ε_z. This fact alone favours the singlet ground state. Secondly, the change of the Madelung potential at the oxygen in-plane orbitals due to the closer and positively charged apical oxygen sites results in the lowering of bare atomic energy levels of planar oxygens [16]. The maximal superconducting temperature T_c is larger for larger values of $|\varepsilon_a - \varepsilon_p|$ [16]. The larger $|\varepsilon_a - \varepsilon_p|$ can be realized by increasing ε_a, not only by decreasing ε_p. So we have shown above that increasing ε_a not only decreases the hole occupancy within apical oxygens but also leads to the increase of T_c.

Finally, we note that doping generates small-polaronic self-trapped local singlets, with the doped hole stabilizing a local distortion of the lattice, if one includes the coupling to the lattice [44, 45]. As a result, the local covalency $\sim t_{pp}$ increases, and the ZR singlets are stabilized, in agreement with our present results. Larger doping stabilizes instead more extended structures not accessible in such small clusters, as domain walls with the doped holes concentrated on the walls. How such domain walls are connected with the phenomenon of high-T_c superconductivity remains to be clarified, but certainly the realistic five-band model considered in this paper deserves more attention in this context.

Acknowledgments

We thank L F Feiner, J H Jefferson, S De Filippo, C Noce, and A Romano for valuable discussions. CL acknowledges the hospitality of the Institute of Physics, Jagellonian University, Cracow. AMO and KR acknowledge the financial support of the Polish Committee of Scientific Research (KBN), Project No 2 P03B 144 08. We also acknowledge the support of the EU PECO grant No CRBCIPDCT940017.

References

[1] Haas K C 1989 *Solid State Physics* vol 42, ed H Ehrenreich and D Turnbull (London: Academic) p 213
[2] Pickett W E 1989 *Rev. Mod. Phys.* **61** 433
[3] Dagotto E 1994 *Rev. Mod. Phys.* **66** 763
[4] Plakida N M 1995 *High-Temperature Superconductivity* (Berlin: Springer)
[5] Czyżyk M T and Sawatzky G A 1994 *Phys. Rev.* B **49** 14 211
[6] Varma C M, Schmitt-Rink S and Abrahams E 1987 *Solid State Commun.* **62** 681
[7] Emery V J 1987 *Phys. Rev. Lett.* **58** 2794
[8] Grant J B and McMahan A K 1992 *Phys. Rev.* B **46** 8440; 1991 *Phys. Rev. Lett.* **66** 488
[9] Nücker N, Romberg H, Xi X X, Fink J, Gegenheimer B and Zhao Z X 1989 *Phys. Rev.* B **39** 6619
[10] Chen C T, Tjeng L H, Kwo J, Kao H L, Rudolf P, Sette F and Fleming R M 1992 *Phys. Rev. Lett.* **68** 2543
[11] Kamimura H 1988 *Int. J. Mod. Phys.* B **1** 699
[12] Weber W 1988 *Z. Phys.* B **70** 323
[13] Cox D L, Jarrell M, Jayaprakash C, Krishnamurthy H R and Deisz J 1989 *Phys. Rev. Lett.* **62** 2188

[14] Nickel J H, Morris D M and Ager J W III 1993 *Phys. Rev. Lett.* **70** 81
[15] de Leeuw D M, Groen W A, Feiner L F and Havinga E E 1990 *Physica C* **166** 133
[16] Ohta Y, Tohyama T and Maekawa S 1991 *Phys. Rev.* B **43** 2968
[17] Di Castro C, Feiner L F and Grilli M 1991 *Phys. Rev. Lett.* **66** 3209
[18] Feiner L F, Grilli M and Di Castro C 1992 *Phys. Rev.* B **45** 10 647
[19] Feiner L F, Jefferson J H and Raimondi R 1996 *Phys. Rev. Lett.* **76** 4939
[20] Zhang F C and Rice T M 1988 *Phys. Rev.* B **37** 3759
[21] Jefferson J H, Eskes H and Feiner L F 1992 *Phys. Rev.* B **45** 7959
[22] McMahan A K, Martin R M and Satpathy S 1988 *Phys. Rev.* B **38** 6650
[23] Hybertsen M S, Schluter M and Christensen N E 1989 *Phys. Rev.* B **39** 9028
[24] Stechel E B and Jennison D R 1988 *Phys. Rev.* B **38** 8873
[25] Mila F 1988 *Phys. Rev.* B **38** 11 358
[26] Lanczos C 1950 *J. Res. NBS* **45** 255
[27] Ralston A 1985 *A First Course in Numerical Analysis* (New York: McGraw-Hill)
[28] Nishimo T 1992 *J. Phys. Soc. Japan* **61** 3651
[29] Lin H Q and Gubernatis J E 1993 *Comput. Phys.* **7** 400
[30] Fujimori A 1989 *Phys. Rev.* B **39** 793
[31] Eskes H, Tjeng L H and Sawatzky G A 1990 *Phys. Rev.* B **41** 288
[32] Ovchinnikov S G 1991 *Mod. Phys. Lett.* B **5** 531
[33] Eskes H, Sawatzky G A and Feiner L F 1989 *Physica* C **160** 424
[34] Tohyama T and Maekawa S 1990 *Physica* B **165+166** 1019
[35] Stephan W H, von der Linden W and Horsch P 1989 *Phys. Rev.* B **39** 2924
[36] Hirsch J E, Tang S, Loh E Jr and Scalapino D 1989 *Phys. Rev. Lett.* **60** 1668
[37] Dutka J and Oleś A M 1990 *Phys. Rev.* B **42** 105
[38] Dutka J and Oleś A M 1991 *Phys. Rev.* B **43** 5622
[39] Pellegrin E, Nücker N, Fink J, Molodtsov S L, Gutierrez A, Navas E, Strebel O, Hu Z, Domke M, Kaindl G, Uchida S, Nakamura Y, Markl J, Klauda M, Saemann-Ischenko G, Krol A, Peng J L, Li Z Y and Green R L 1993 *Phys. Rev.* B **47** 3354
[40] Zaanen J and Oleś A M 1988 *Phys. Rev.* B **37** 9423
[41] Raimondi R, Jefferson J H and Feiner L F 1966 *Phys. Rev.* B **53** 8774
[42] Zaanen J, Sawatzky G A and Allen J W 1985 *Phys. Rev. Lett.* **55** 418
[43] Meinders M B J, Eskes H and Sawatzky G A 1993 *Phys. Rev.* B **48** 3916
[44] Dobry A, Greco A, Lorenzana J and Riera J 1994 *Phys. Rev.* B **49** 505
[45] Zaanen J and Littlewood P 1994 *Phys. Rev.* B **50** 7222